Supporting Information

Integration of a Screening-Guided Near-Infrared Aptasensor into a Portable Platform for Quantitative On-Site Detection of N^1-Methyladenosine

Qi Pang[a], Dandan Zhang[b], Ruilin Ma[d], Wuduo Zhao[a,b], Xinyue Cao[a], Zhongyang Huang[b], Tuanjie Huang[c*], and Jiaheng Zhang[a,b*]

[a] School of Ecology and Environment, Zhengzhou University, Zhengzhou 450001, China

[b] College of Chemistry, Zhengzhou University, Zhengzhou 450001, China

[c] Department of Clinical Laboratory, The First Affiliated Hospital of Zhengzhou University, Zhengzhou, 450001, China

[d] Hydrology and Water Resources Monitoring and Forecasting Center of Henan Province 450001, China

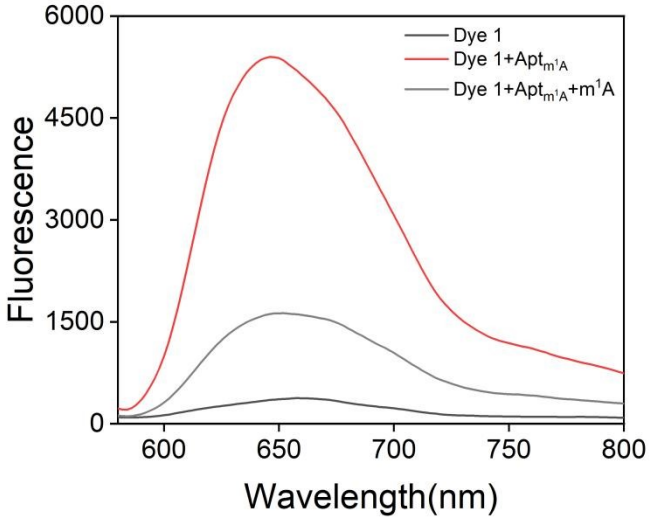

Fig. S1 Fluorescence spectra of Crystal Violet (Ex: 540 nm / Em: 650 nm) binding to the Apt$_{m}{}^{1}$A and m^{1}A competition in Tris buffer.

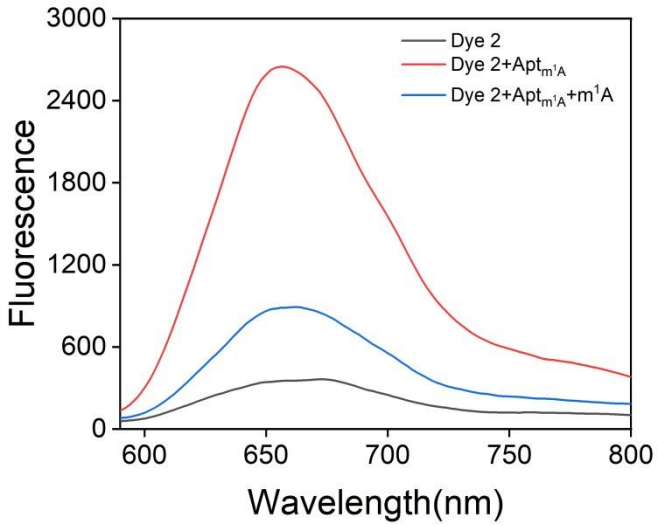

Fig. S2 Fluorescence spectra of Ethyl Violet (Ex: 550 nm / Em: 650 nm) binding to the Apt$_{m}{}^{1}$A and m^{1}A competition in Tris buffer.

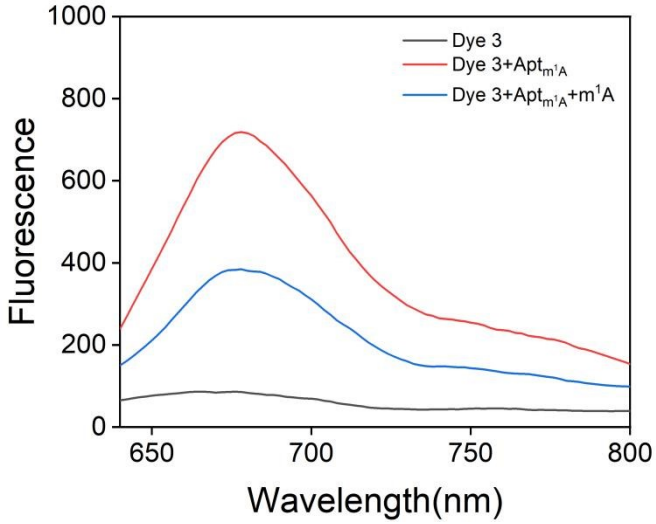

Fig. S3 Fluorescence spectra of Methyl Green zinc chloride salt (Ex: 600 nm / Em: 670 nm) binding to the Apt$_m{}^1{}_A$ and m^{1}A competition in Tris buffer.

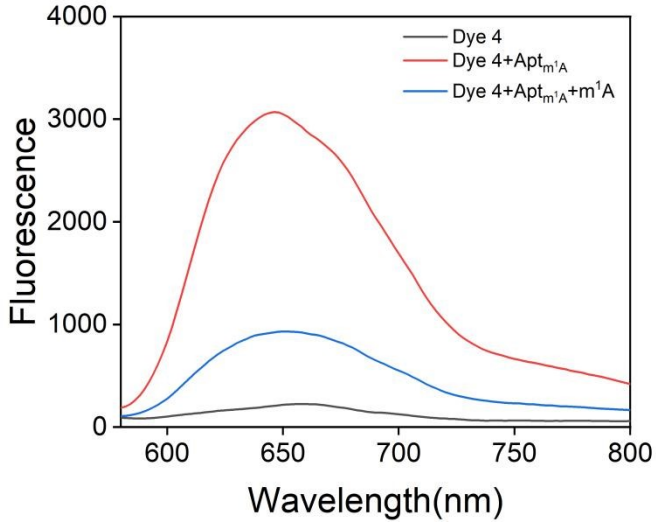

Fig. S4 Fluorescence spectra of Solvent Violet 8 (Ex: 540 nm / Em: 630 nm) binding to the Apt$_m{}^1{}_A$ and m^{1}A competition in Tris buffer.

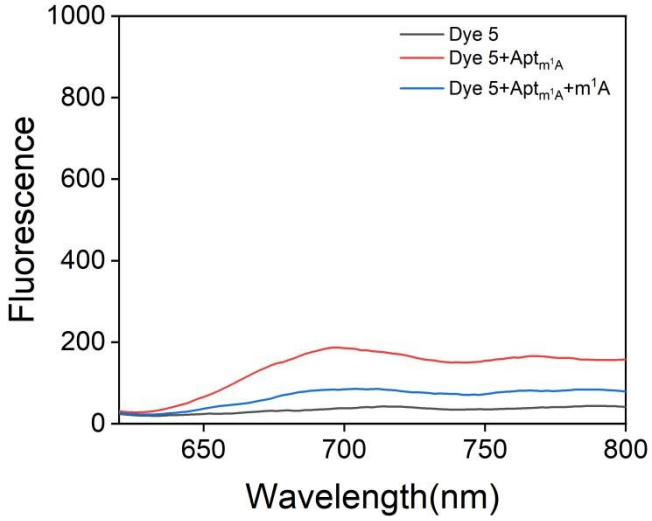

Fig. S5 Fluorescence spectra of Basic Blue 26 (Ex: 585 nm / Em: 686 nm) binding to the Apt$_{m}{}^{1}{}_{A}$ and m^{1}A competition in Tris buffer.

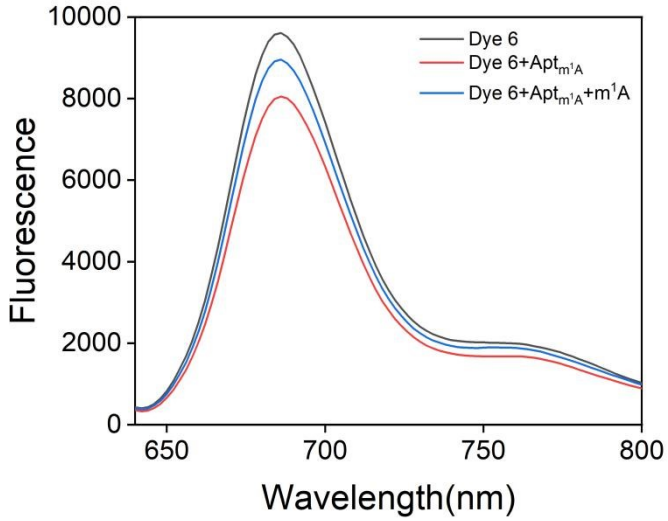

Fig. S6 Fluorescence spectra of Basic Blue 11 (Ex: 600 nm / Em: 686 nm) binding to the Apt$_{m}{}^{1}{}_{A}$ and m^{1}A competition in Tris buffer.

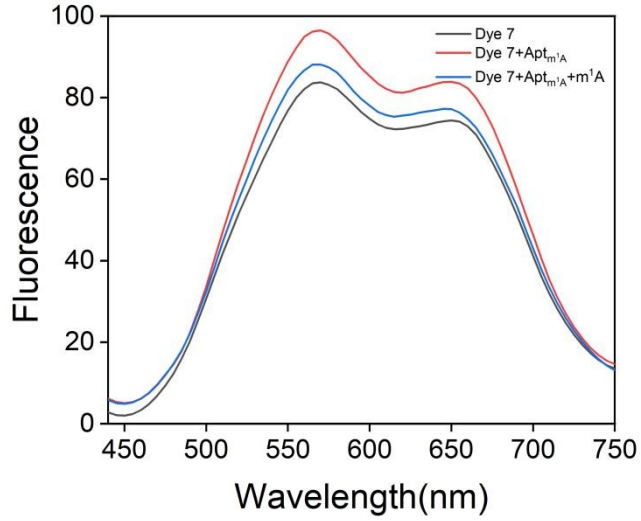

Fig. S7 Fluorescence spectra of Basic Coumarin 6 (Ex: 400 nm / Em: 570 nm) binding to the Apt$_{m}{}^{1}$A and m^{1}A competition in Tris buffer.

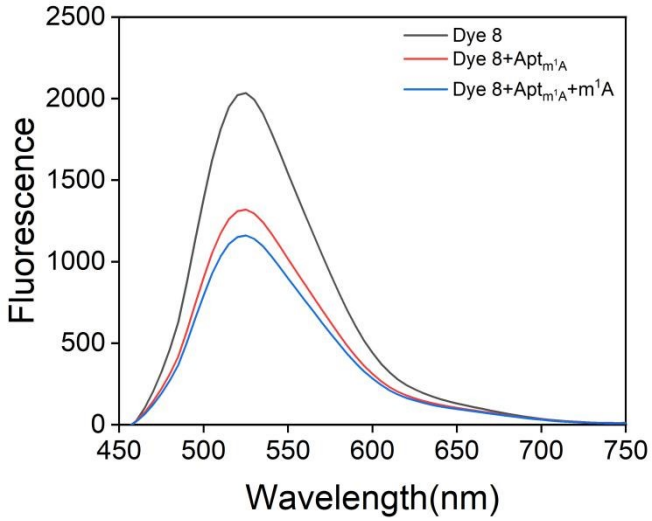

Fig. S8 Fluorescence spectra of S2153 (Ex: 410 nm / Em: 530 nm) binding to the Apt$_{m}{}^{1}$A and m^{1}A competition in Tris buffer.

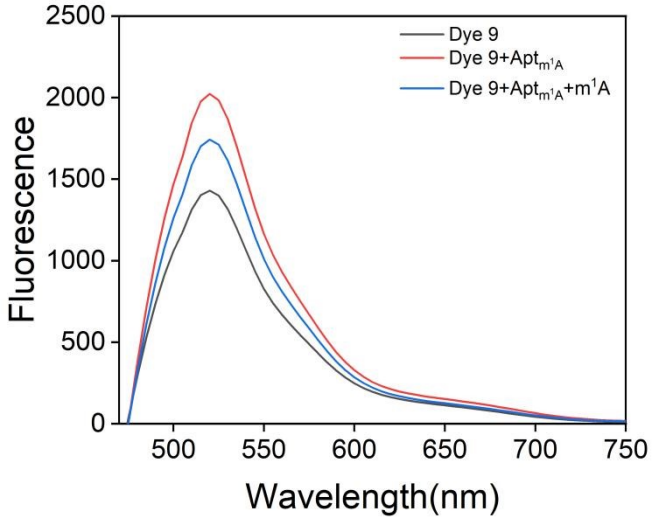

Fig. S9 Fluorescence spectra of 3OUMARIN 525 (Ex: 430 nm / Em: 530 nm) binding to the $Apt_m{}^1{}_A$ and m^1A competition in Tris buffer.

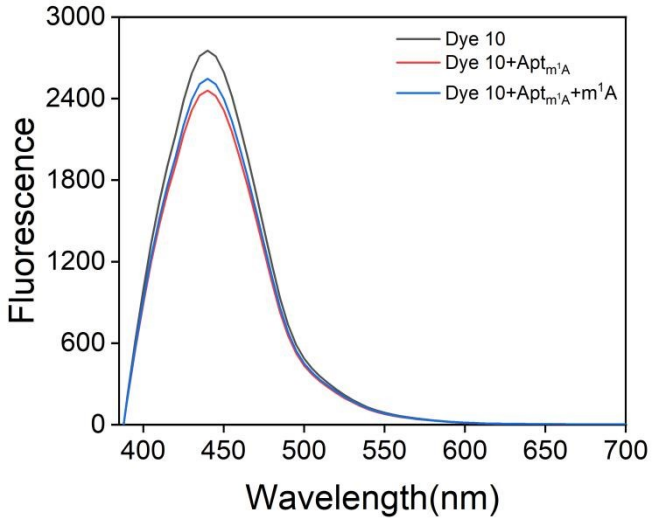

Fig. S10 Fluorescence spectra of Coumarin 478 (Ex: 430 nm / Em: 530 nm) binding to the $Apt_m{}^1{}_A$ and m^1A competition in Tris buffer.

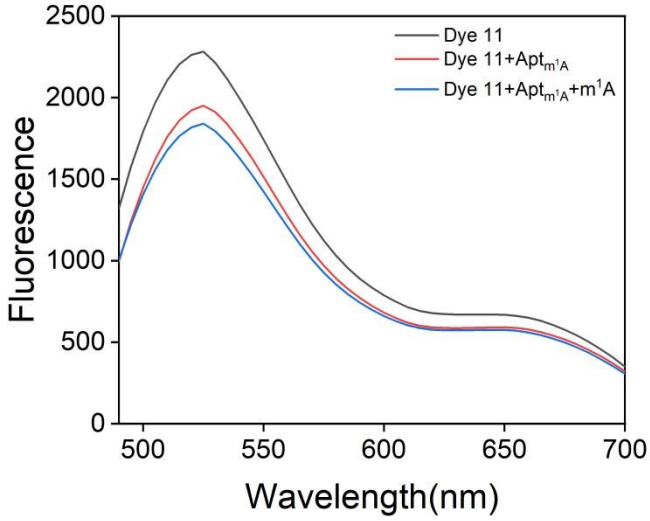

Fig. S11 Fluorescence spectra of Exciton Coumarin 545 (Ex: 450 nm / Em: 520 nm) binding to the Apt$_{m}{}^{1}{}_{A}$ and m^{1}A competition in Tris buffer.

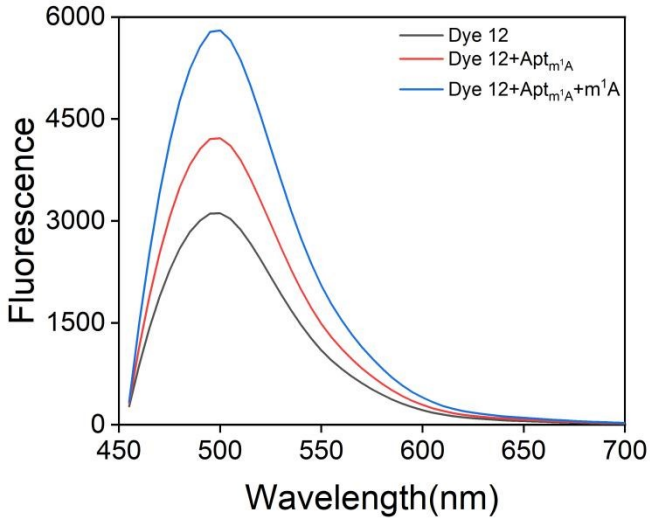

Fig. S12 Fluorescence spectra of Coumarin 30 (Ex: 415 nm / Em: 500 nm) binding to the Apt$_{m}{}^{1}{}_{A}$ and m^{1}A competition in Tris buffer.

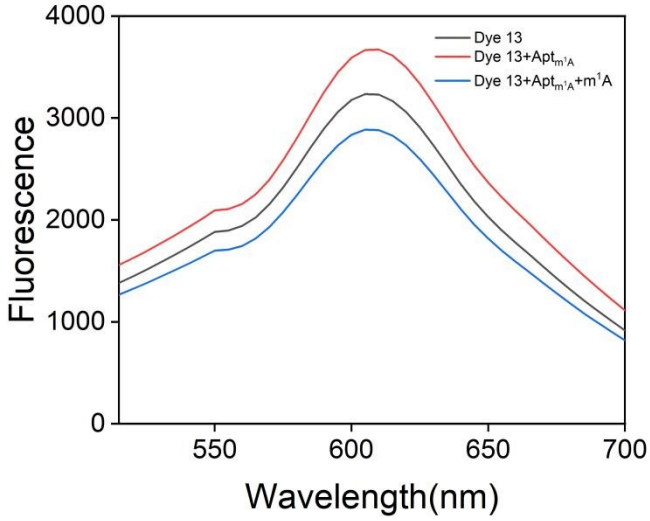

Fig. S13 Fluorescence spectra of Coumarin 545T (Ex: 475 nm / Em: 605 nm) binding to the Apt_{m^1A} and m^{1}A competition in Tris buffer.

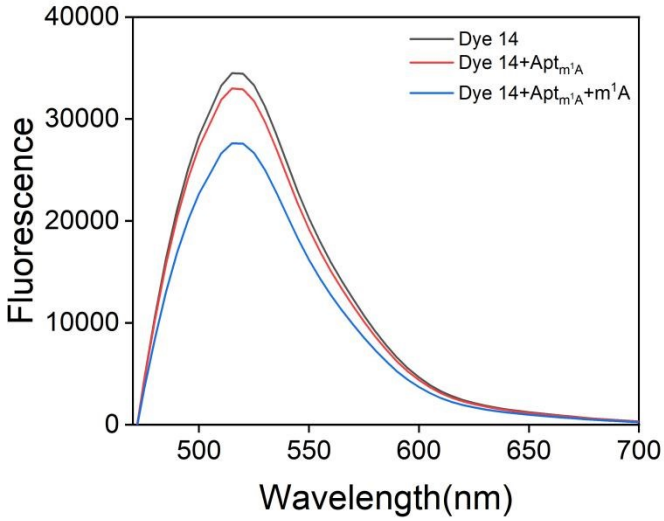

Fig. S14 Fluorescence spectra of Coumarin 510 (Ex: 430 nm / Em: 520 nm) binding to the Apt_{m^1A} and m^{1}A competition in Tris buffer.

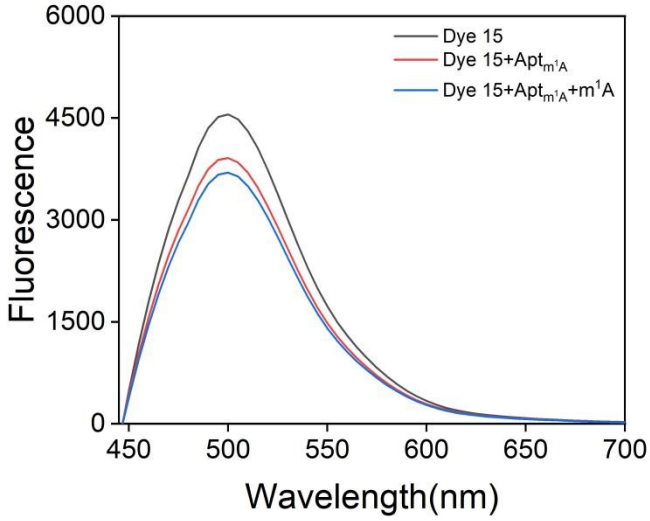

Fig. S15 Fluorescence spectra of Coumarin 73 (Ex: 405 nm / Em: 515 nm) binding to the Apt$_{m}{}^{1}{}_{A}$ and m^{1}A competition in Tris buffer.

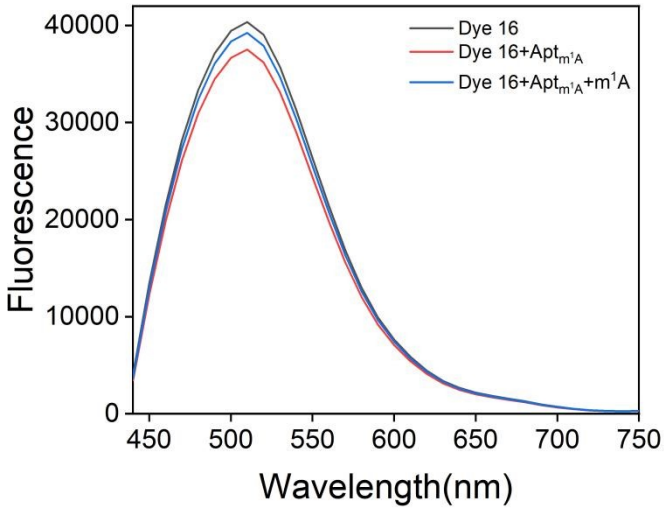

Fig. S16 Fluorescence spectra of Coumarin 151 (Ex: 400 nm / Em: 500 nm) binding to the Apt$_{m}{}^{1}{}_{A}$ and m^{1}A competition in Tris buffer.

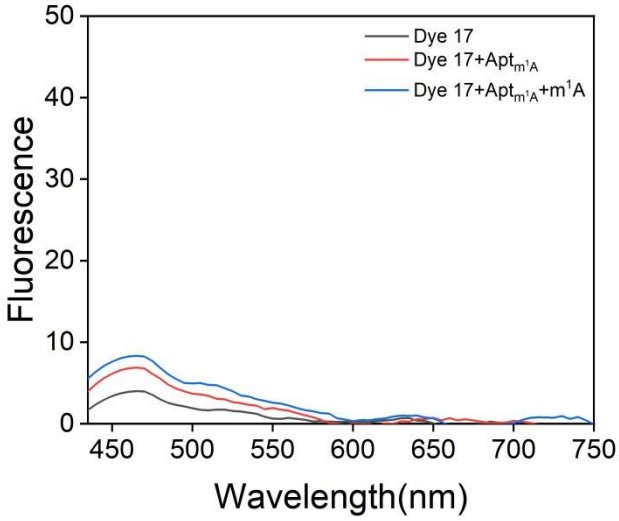

Fig. S17 Fluorescence spectra of 3',6'-Dimethoxyfluoran (Ex: 395 nm / Em: 465 nm) binding to the Apt$_{m}{}^{1}{}_{A}$ and m^{1}A competition in Tris buffer.

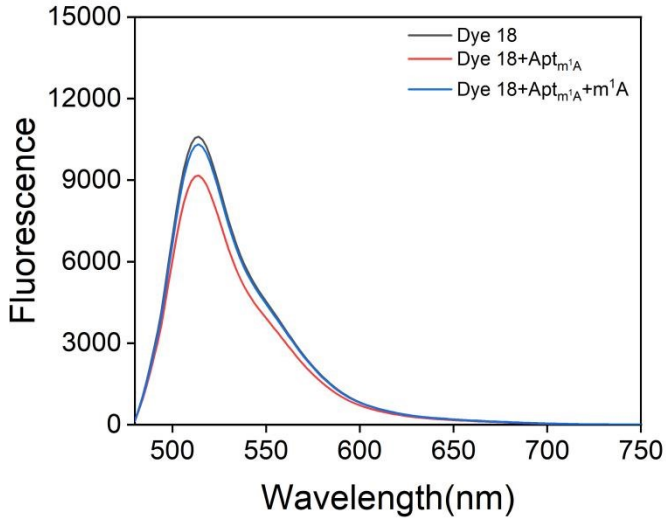

Fig. S18 Fluorescence spectra of Fluorexon (Ex: 440 nm / Em: 520 nm) binding to the Apt$_{m}{}^{1}{}_{A}$ and m^{1}A competition in Tris buffer.

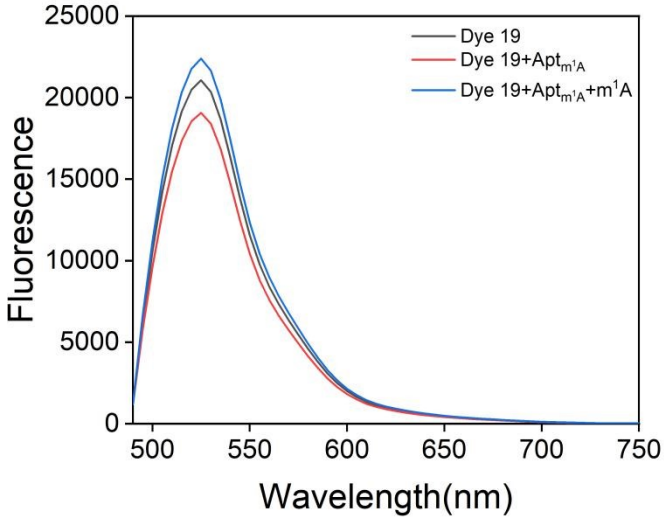

Fig. S19 Fluorescence spectra of 6-Carboxyfluorescein (Ex: 450 nm / Em: 530 nm) binding to the Apt$_{m}{}^{1}{}_{A}$ and m^{1}A competition in Tris buffer.

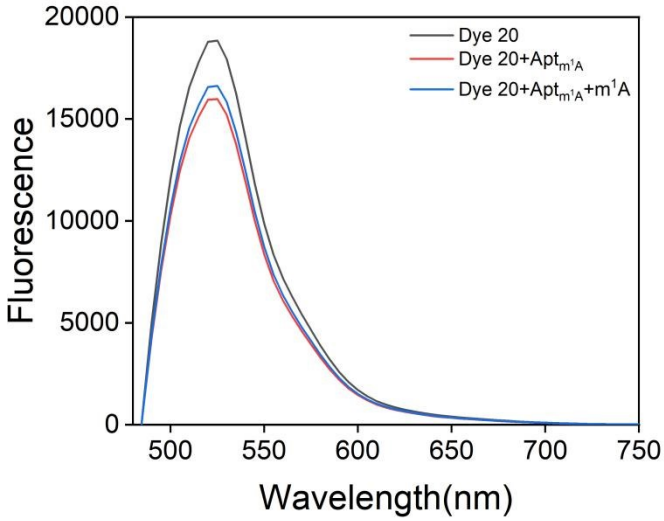

Fig. S20 Fluorescence spectra of Fluorescein (Ex: 440 nm / Em: 530 nm) binding to the Apt$_{m}{}^{1}{}_{A}$ and m^{1}A competition in Tris buffer.

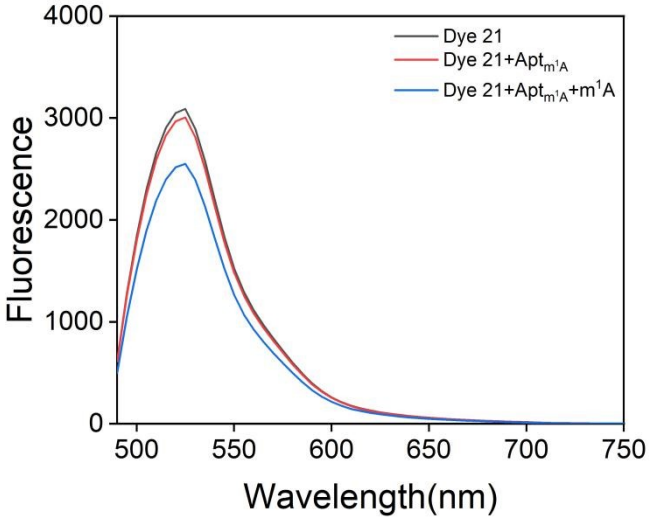

Fig. S21 Fluorescence spectra of Fluorescein Sodium (Ex: 420 nm / Em: 530 nm) binding to the Apt$_{m}{}^{1}{}_{A}$ and m^{1}A competition in Tris buffer.

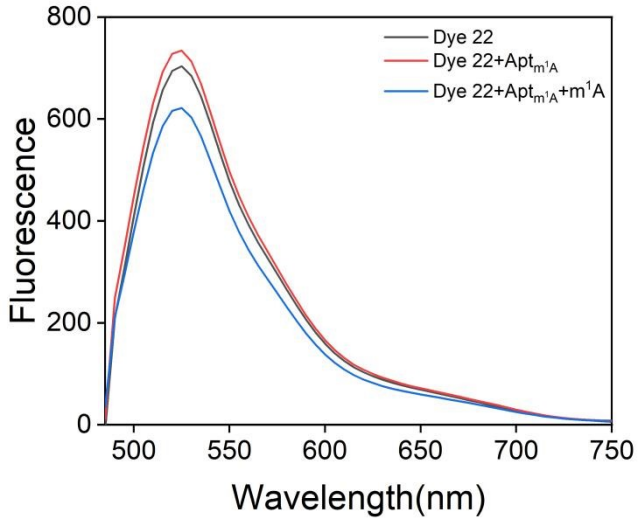

Fig. S22 Fluorescence spectra of 3',6'-Dichlorofluoran (Ex: 410 nm / Em: 530 nm) binding to the Apt$_{m}{}^{1}{}_{A}$ and m^{1}A competition in Tris buffer.

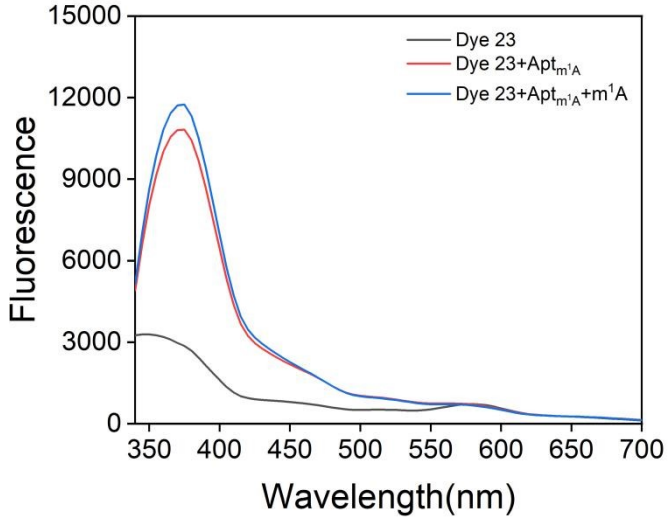

Fig. S23 Fluorescence spectra of 2-(2-aminoethyl) Rhodamine B amide (Ex: 295 nm / Em: 375 nm) binding to the Apt$_{m}{}^{1}{}_{A}$ and m^{1}A competition in Tris buffer.

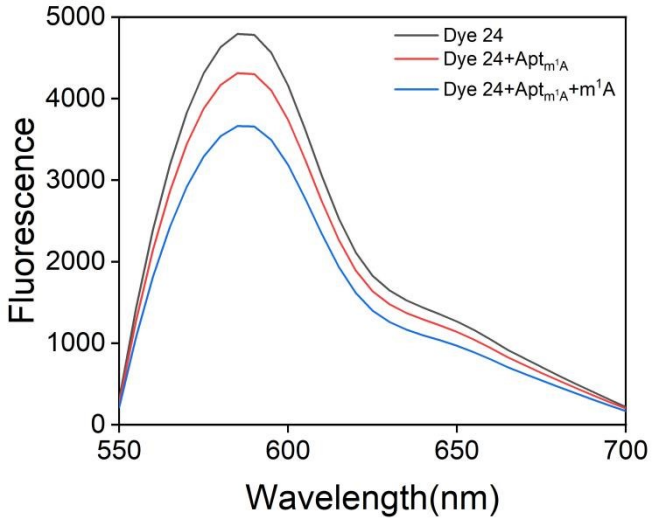

Fig. S24 Fluorescence spectra of Sulforhodamine B (Ex: 510 nm / Em: 595nm) binding to the Apt$_{m}{}^{1}{}_{A}$ and m^{1}A competition in Tris buffer.

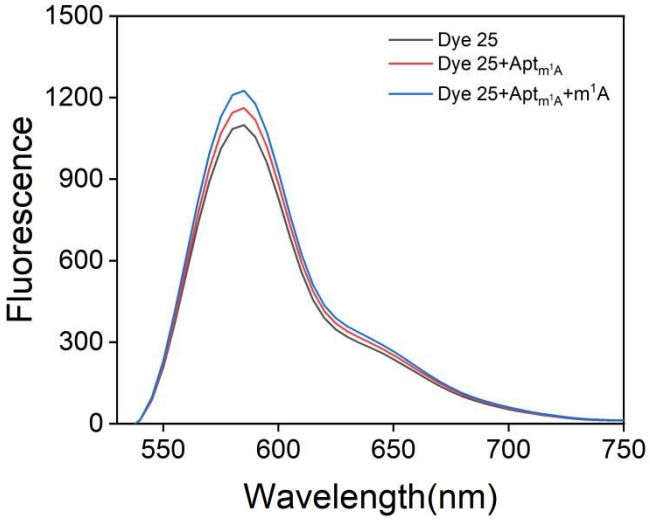

Fig. S25 Fluorescence spectra of Rhodamine B (Ex: 420 nm / Em: 590 nm) binding to the Apt$_{m}{}^{1}{}_{A}$ and m^{1}A competition in Tris buffer.

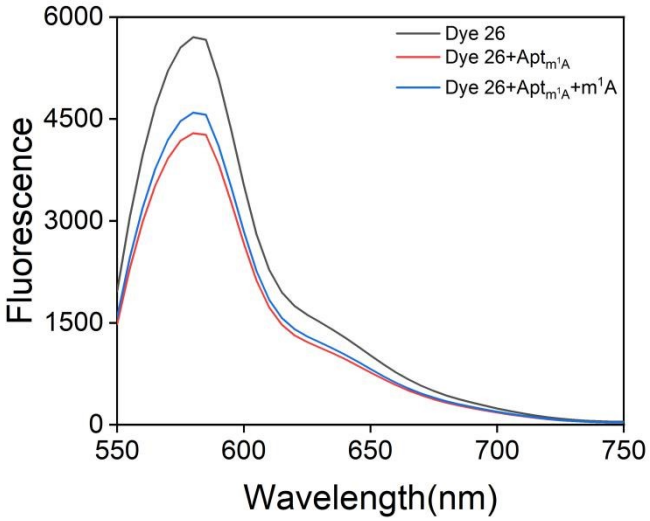

Fig. S26 Fluorescence spectra of Pyronin B (Ex: 510 nm / Em: 580 nm) binding to the Apt$_{m}{}^{1}{}_{A}$ and m^{1}A competition in Tris buffer.

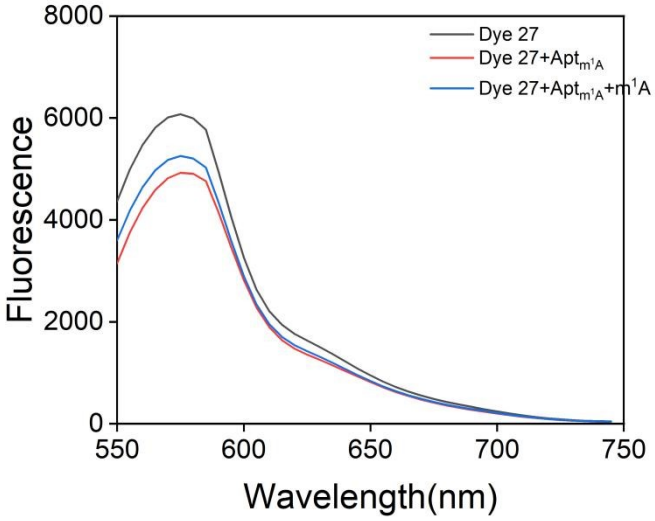

Fig. S27 Fluorescence spectra of Pyronin Y (Ex: 510 nm / Em: 580 nm) binding to the Apt$_{m}{}^{1}{}_{A}$ and m^{1}A competition in Tris buffer.

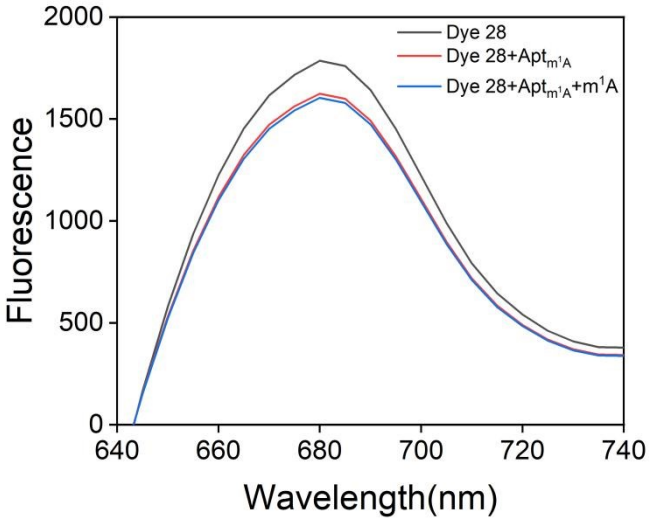

Fig. S28 Fluorescence spectra of OXAZINE 1 (Ex: 600 nm / Em: 680 nm) binding to the Apt$_{m}{}^{1}{}_{A}$ and m^{1}A competition in Tris buffer.

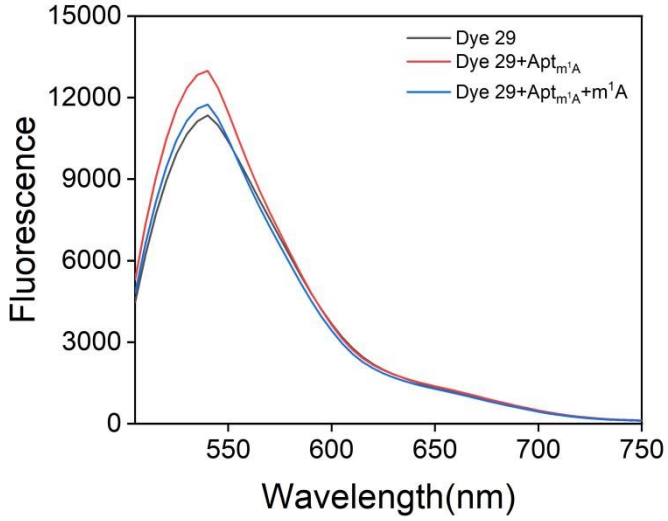

Fig. S29 Fluorescence spectra of Basic Orange 14 (Ex: 465 nm / Em: 530 nm) binding to the Apt$_{m}{}^{1}{}_{A}$ and m^{1}A competition in Tris buffer.

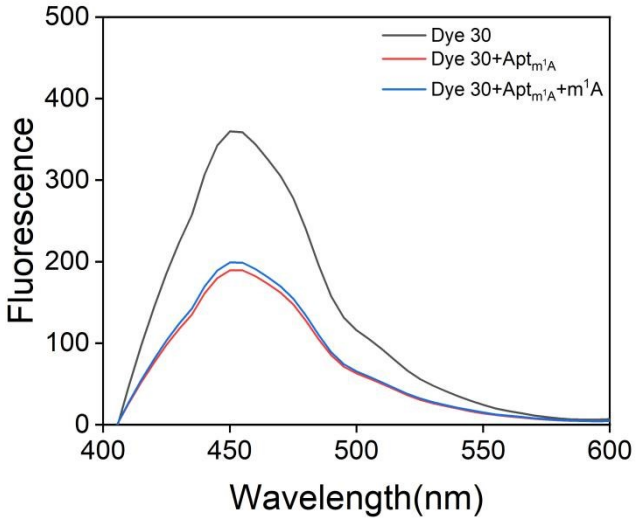

Fig. S30 Fluorescence spectra of 9-Aminoacridine (Ex: 250 nm / Em: 460 nm) binding to the Apt$_{m}{}^{1}{}_{A}$ and m^{1}A competition in Tris buffer.

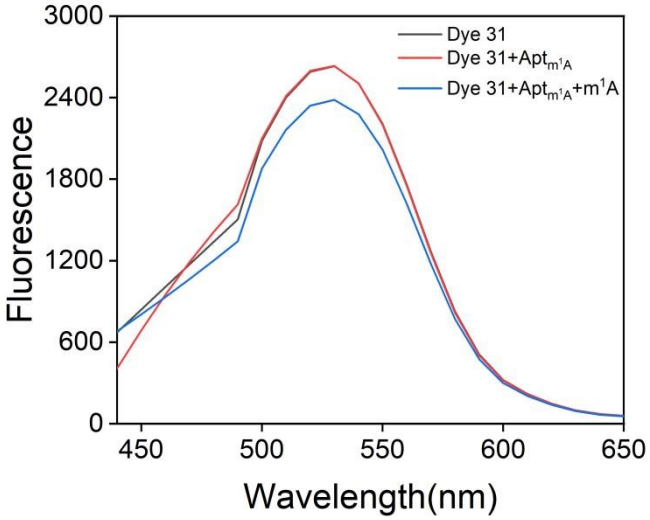

Fig. S31 Fluorescence spectra of BODIPY(R) 493/503 (Ex: 380 nm / Em: 520 nm) binding to the Apt$_m{}^1{}_A$ and m^{1}A competition in Tris buffer.

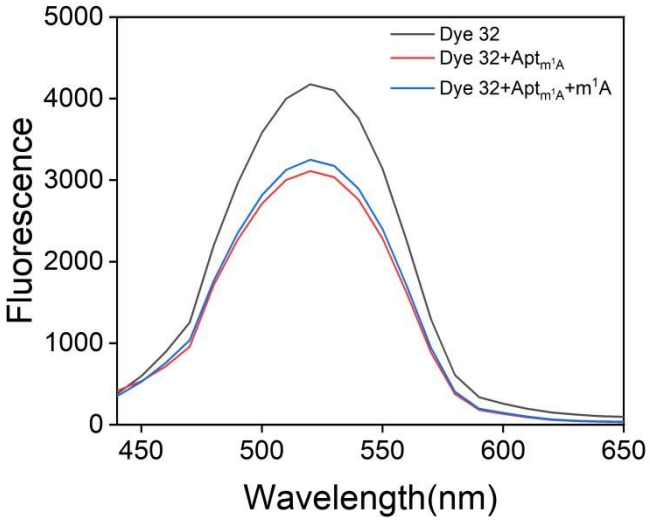

Fig. S32 Fluorescence spectra of 8-Phenyl-BODIPY 505/515 (Ex: 360 nm / Em: 520 nm) binding to the Apt$_m{}^1{}_A$ and m^{1}A competition in Tris buffer.

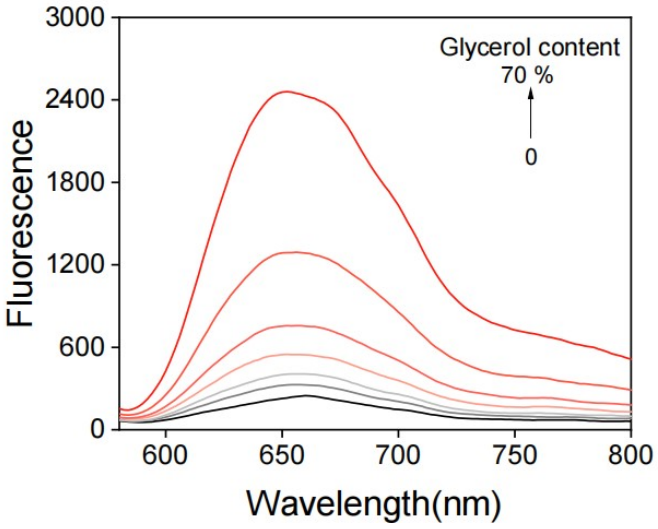

Fig. S33 Fluorescence spectra of CV in a mixture of Tris buffer and glycerol.

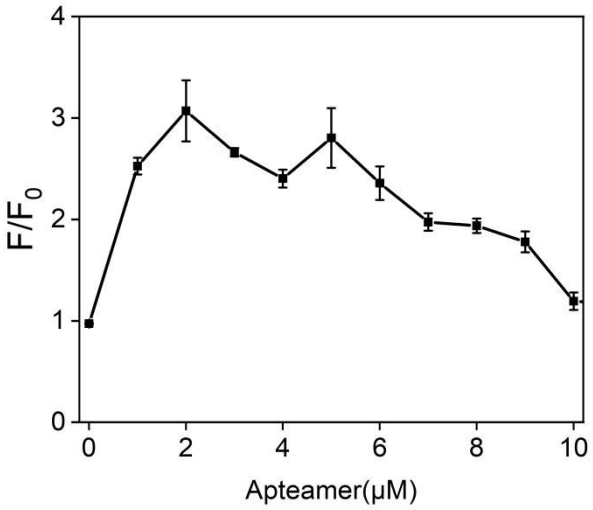

Fig. S34 The fluorescence intensity of mixtures containing CV at 10 μM bound to different concentrations of aptamers, relative to the fluorescence of the same mixture supplemented with m^1A (10 μM).

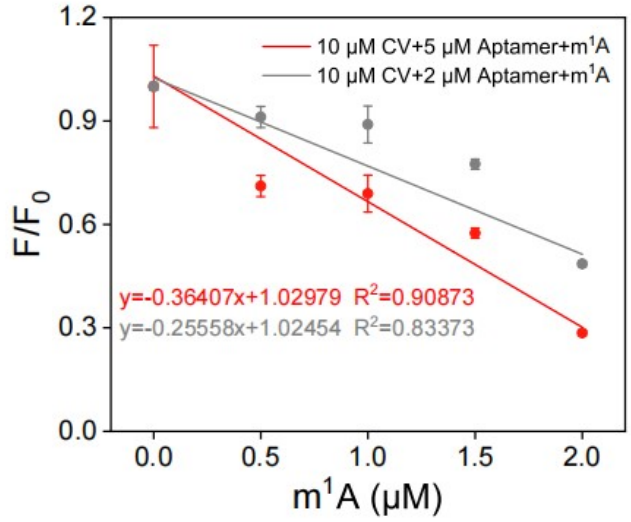

Fig. S35 Linear response in the concentration range of 0–2 μM at different aptamer concentrations.

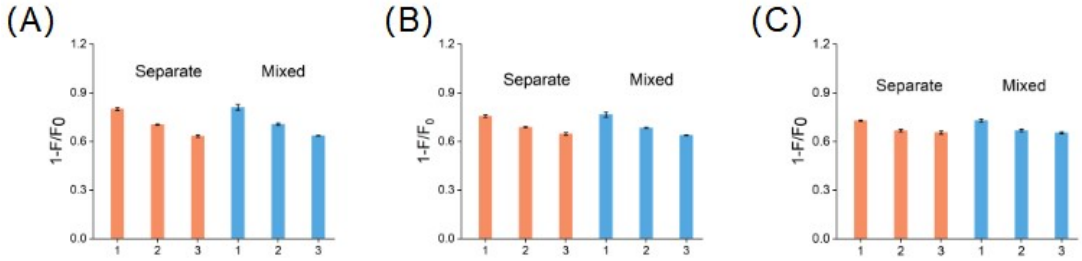

Figure S36. Storage stability of CV, Apt_{m^1A}, and the CV-Apt_{m^1A} complex for m^1A sensing after storage -20 °C (A), 4 °C (B), and 25 °C (C) for 1, 2 and 3 days. In the "separate" mode, CV and Apt_{m^1A} were stored independently and mixed before testing; In the "mixed" mode, the pre-formed complex was stored prior to measurement.

Sample	Added（μM	Found（μM）	Recovery（%）
human urine	0.4	0.356	89.1
	0.6	0.606	101.1
	0.6.	0.684	85.5
	1.0	1.095	109.5

Table S1. The application of sensing method to spiked human urine samples.

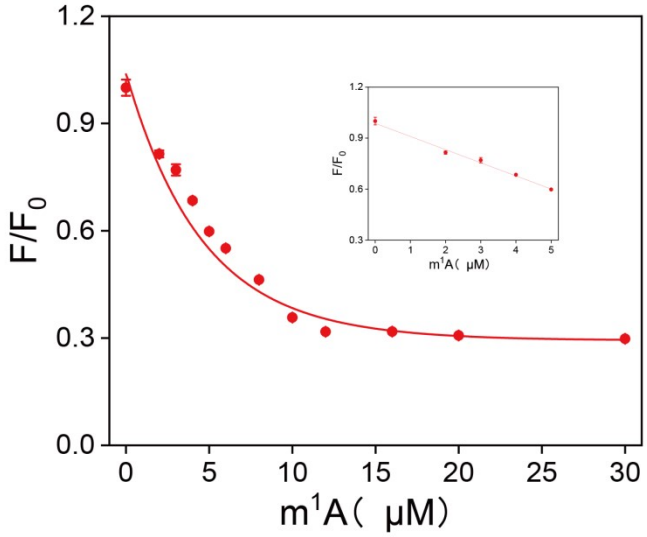

Fig. S37 Fluorescence intensity of CV-Apt$_{m^1A}$ complexes measured by POCT device at different m^{1}A concentrations.

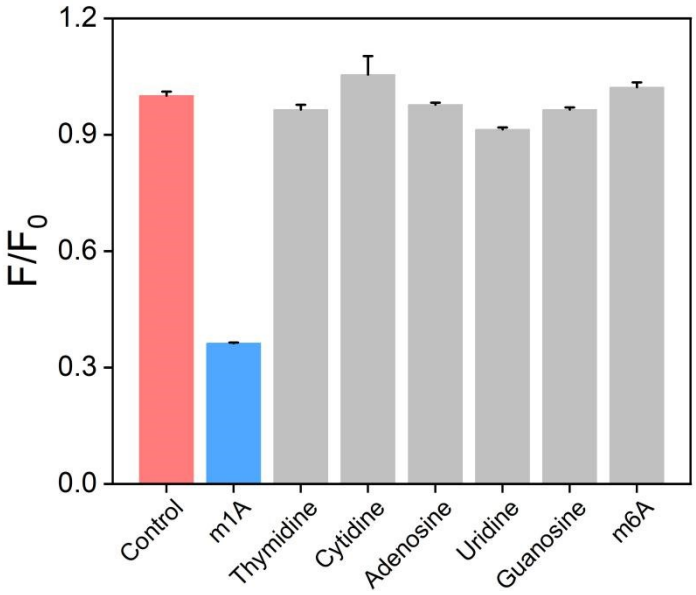

Fig. S38 Selectivity of CV-Apt$_{m^1A}$ complexes for m^{1}A measured by POCT device.